ON THE ADOPTION OF HYBRID RANS-LES TURBULENCE MODELLING TECHNIQUE FOR AEROELASTIC PROBLEMS – IFASD 2017

Marcello Righi[1]

[1]School of Engineering
Zurich University of Applied Sciences
Technikumstrasse 9, CH-8401 Winterthur
marcello.righi@zhaw.ch

Keywords: turbulence modelling, RANS, LES, hybrid RANS-LES, unsteady aerodynamics, structural dynamics, aeroelasticity

Abstract: This paper investigates hybrid RANS-LES turbulence modelling in real-life aeroelastic problems. The analysis is based on the author's calculations carried out in the framework of the Second Aeroelastic Prediction Workshop, those requested by the GARTEUR Action Group AG54, codenamed RALESIN (`www.ag54-garteur.online`), and the assessment of a few additional test cases, introduced especially to improve the understanding of hybrid models. Unsurprisingly, the analysis shows that hybrid turbulent methods can be very accurate but that quality may quickly degrade as the calculations parameters (spatial and temporal resolution, subgrid filter and turbulence model) move away from optimum values.

NOMENCLATURE

DES	=	Detached Eddy Simulation
DDES	=	Delayed Detached Eddy Simulation
FRF	=	Frequency Response Function
LES	=	Large Eddy Simulation
PSD	=	Power Spectral Density
RANS, URANS	=	(Unsteady) Reynolds Averaged Navier Stokes
SA	=	Spalart-Allmaras turbulence model
SA-DDES	=	DDES model based on the SA turbulence model
SGS	=	SubGrid Scale

INTRODUCTION

For many engineering studies involving fluid mechanics at high Reynold number, the RANS approach is virtually the only viable option. However, it is recognized that RANS accuracy may degrade in the presence of some physical phenomena [1, 2]. In particular, RANS solutions may become questionable as soon as large unsteady turbulent scales of motion appear. Approaches such as LES and WMLES, which aim at explicitly resolving a substantial amount of the turbulent inertial subrange, are more accurate and robust. However, the associated computational demand may still be beyond reach for many users.

Hybrid RANS-LES turbulence models were introduced [3] precisely to exploit LES accuracy and RANS affordability. The approach appears as a natural extension of RANS methods for industrial CFD. The idea consists in using both approaches at the same time: flow regions with larger turbulent scales of motions are explicitly resolved (LES) whereas regions with smaller ones are modelled (RANS). The criteria followed in order to divide the computational domain into RANS and LES vary among the different approaches [4]. The overall accuracy of the method strongly relies on LES; the relevance of hybrid modelling becomes more evident as computational resources become more affordable.

Hybrid RANS-LES turbulence modelling can be seen as a general framework which groups several techniques, as can be gathered e.g. from the review by Frölich and von Terzi [4] as well as from the proceedings of the bi-annual dedicated symposium [5–7]. Note, however, that within the aeronautical community the *DES* – Detached Eddy Simulation [3] – is often preferred to other techniques, maybe as a consequence of the preference for the Spalart-Allmaras RANS model [8]. The latter is very much appreciated for its robustness, economy and overall accuracy in shear dominated flows. Due to its simple underlying physical model, this model is not always capable of generating consistent Reynolds stress models in the presence of different type of flows, such as separated regions. For this reason, coupling the Spalart-Allmaras model to an LES model seems to be quite advantageous, exploiting its economy and robustness and allowing the LES branch to improve accuracy. The DDES (Delayed DES) option [9] is probably the most popular hybrid approach, normally coupled to the SA and to the k-ω RANS models.

Hybrid models represent an interesting resource also for aeroelasticians [10]. Possibly even more than for other analysts, since the most critical aeroelastic assessments often require the analysis of non-linear aerodynamics. It might be the case of flight points at the margin of aircraft flight envelope or the analysis of flow instabilities in compressors. Moreover, aeroelasticians often calculate in time-domain and rely on time-accurate simulations, regardless of turbulence model. Switching to hybrid RANS-LES models could then be less demanding in terms of additional computing requirements than in other cases. The added-value of hybrid analysis include a more accurate assessment of the equilibrium solution (i.e. the solution to the "static aeroelastic" problem), consequently more accurate linear stability analysis but also the means to investigate non-linear phenomena such as LCOs. It is worth noting that the last Aeroelastic Prediction Workshop proposed a test case, dominated by separated flow, inviting the participants to adopt hybrid techniques [11–14].

This paper continues in Section 2, where the specific requirements are reviewed, Section 3 where some test cases are discussed and Section 4 with the conclusions.

ADDITIONAL COSTS WITH RESPECT TO RANS ASSOCIATED WITH HYBRID MODELLING

Costs Associated with CPU and Workload

That hybrid modelling imposes non-negligible computational costs and that the calculations set-up may become quite different from a conventional RANS simulation is well known, as it is evident from the Guide written by Spalart in the early years of this technique [15]. It is also well known that the additional costs do not only affect computations but can be related to the whole assessment process, namely:

1. Substantially higher meshing efforts are requested, in order to (i) assign different spatial resolution to different (RANS / LES) regions, (ii) prevent grid-induced RANS to LES switching, (iii) adjust grid size to turbulent lengthscales in LES regions,
2. Calculations may become costly, partly due to grid size but especially because minimum values are imposed on both temporal resolution and the overall duration:
   (a) temporal resolution is necessary to exploit spatial resolution and let resolved turbulent structures evolve properly; this requirement often translates into a "CFL = 1" condition.
   (b) overall duration depends on the need to time-average turbulent quantities but also on the lower frequencies involved in the problem,
   (c) a problem involving a full-scale aircraft wing may require time steps as small as 10^{-6} or 10^{-7} seconds and an overall duration the order of 1 second, i.e. sufficient to capture the effects of structural modes with eigenfrequencies of a few Hertz.
3. Post-processing is much more demanding, as the resolved turbulence must be time-averaged and checked for consistency.

It would be very difficult to quantify the additional costs as they vary strongly with the characteristics of the test case. However, it would not be unreasonable to consider one or two orders of magnitude for both CPU and personnel budgets.

Costs Associated with the Fact that Hybrid Models are still being developed

Hybrid turbulence modelling techniques, even the popular SA-DDES, still have not reached a maturity level such, that industrial applications can be routinely run by non-expert users. Their application may therefore still provide unexpected results whose analysis may generate additional costs.

In particular, the following aspects are still under investigation:

1. The behaviour of hybrid models in the RANS-LES region, the so-called "gray-area" is not well understood; anticipated or delayed switching to LES may lead to non-physical behavior and be detrimental to the overall accuracy.
2. Results are still very much dependent on spatial resolution [15], which is expected, with grid convergence not always successful[1]
3. Results are still dependent on temporal resolution [15], which is also expected. Note that most hybrid models do not compensate insufficient resolved turbulence – caused by too large a time step – with additional eddy viscosity (from the RANS model).
4. Many test cases are solved and published by means of higher-order schemes and high-quality structured grids. How the quality of results degrade when using conventional second-order schemes and unstructured grids is difficult to assess.

Note that when hybrid RANS-LES methods are inaccurate or fail, it happens because the LES regions are prevented to develop properly. In this case, the insufficient (overall) turbulence may lead to unphysical phenomena such as separation of the boundary layer or excessive fluctuations in response to excitation, as happens in one of the test cases described in section 3.

[1] It must be noted that the concept of *grid convergence* may lose its original meaning when applied to hybrid modelling.

NUMERICAL EXPERIMENTS

Numerical Method

Most of the results presented in this paper have been obtained with the solver SU2. The SU2 software suite [16–18] is an open-source collection of software tools written in C++ and Python for performing multi-physics simulation and design. It is built specifically for the analysis of partial differential equations (PDEs) and PDE-constrained optimization problems on unstructured meshes with state-of-the-art numerical methods, and it is particularly well suited for aerodynamic shape design. The initial applications of the suite were mostly in aerodynamics, but through the initiative of users and developers around the world, SU2 is now being used for a wide variety of problems beyond aeronautics, including automotive, naval, and renewable energy applications, to name a few. In all calculations presented convective fluxes were modelled according to Roe's scheme [19] with the Venkatakrishnan limiter [20]. The standard dual time stepping was used in all cases. The Krylov problem was solved with FGMRES method and the LU–SGS preconditioner. No multi–grid acceleration was used.

RANS simulations have used the Spalart-Allmaras model [8]. Hybrid simulations have used the SA-DDES model [9]. The so-called ZDES "gray area mitigation" proposed by Deck [21] has been systematically used in all hybrid calculations. The implementation of the hybrid models in SU2 has been completed by E. Molina of ITA, Brazil. All details can be found in IFASD2017 paper N. 134, as well as in the corresponding paper accepted to AVIATION 2017.

Most calculations have been carried out with Roe scheme. The choice might be questioned but it was necessary for robustness and stability while testing the new models and grids. Most grids have been generated by the author and by E. Molina.

Test Cases and Rationale

The following test cases are presented:

1. Dynamic Stall, VR12 Aerofoil [22]: this test case is an example of how a hybrid model can outperform the RANS model with the same spatial and temporal resolution,
2. Shock Buffeting OAT15A Aerofoil [23]: this test case is an example where the hybrid model has the potential to improve RANS accuracy but much depends on the settings,
3. Forced Oscillations, BSCW Supercritical Wing, Second AIAA Aeroelastic Prediction Workshop, Test Case 3 [24]: this case requires an even more demanding analysis of the flow in order to correctly set up the hybrid simulation.

Dynamic Stall VR12 Airfoil

This section proposes a test case where hybrid modelling provide more accurate predictions then RANS with the same spatial and temporal resolutions. Dynamic stall is a classical test case characterized by attached and separated flow regions and is a good candidate for testing hybrid models. The test case chosen for this study is the one published by [22]. The flow is subsonic, Mach 0.3, with a reduced frequency $k = 0.1$. The wind tunnel wing undergoes pitch oscillations with an amplitude of 10 degrees around the angle of attack of 10 degrees. The airfoil is the well-known VR12 developed for rotorcraft, with tab. Calculations have been carried out:

1. the time step is 10^{-5} seconds for all calculations,

2. several pitch revolutions have been simulated until periodic results have been obtained,
3. the grid is structured, contains 4 million elements, and has been designed to guarantee sufficient resolution for the turbulent structures which develop during stall,
4. no efforts have been done to capture transition, calculations are fully turbulent; phenomena like laminar separation bubbles have not been reported by the experimenters.

Lift and moment coefficients are shown in Fig. 4. Measurements are shown in Ref. [22] and not reported here. The comparison shows how the hybrid model comes much closer to the measurements in the stall region. The stall mechanism appears substantially different with the remainder being strongly influenced by the stall behaviour. Resolved turbulent structures are shown in Figures 1, 2 and 3. As expected, the RANS calculation fails to capture much of the turbulent system which is generated by the flow separation, but mainly the largest vortices. On the contrary, DDES calculations show a rich collection of turbulent structures and let us believe that spatial and temporal resolutions are suitable to LES.

Figure 1: Visualization of flow patterns at six different times across stall by means of density gradients. Results obtained from RANS (SA) calculations.

OAT15A Aerofoil

As the calculations and their analysis is still ongoing, the results presented in this section are incomplete.

This test case refers to a well known experiment carried out by Onera [25, 26]. The transonic flow around the OAT15A aerofoil exhibits an evident shock buffeting phenomenon, which can

Figure 2: Visualization of flow patterns at six different times across stall by means of density gradients. Results obtained from SA-DDES calculations.

be captured by numerical experiments [23, 27]. The different studies, and the one by Deck [23] in particular, have shown that RANS models may allow capturing the buffeting motion but hybrid models provide more accurate predictions. The author has performed the calculations with the solver SU2 and the SA-DDES hybrid model with the ZDES mitigation, described earlier in the paper and in IFASD2017 Paper N. 134 by E. Molina. Resolved vortexes are shown in Fig. 6 whereas the PSD of the lift coefficient is presented in Fig. 5. The grid is structured and has approximately 15 million elements. The measured buffeting frequency is slightly below 100 Hz, which corresponds to about 15 Hz in the numerical experiment where the chord is approximately 6 times smaller. The evaluation of the results is still ongoing but the PSD indicate a low frequency for the calculations carried out with angles of attack of 4 and 4.5 degrees. The calculations by Deck [23] captured buffeting at an angle of attack of 3.5 degrees, which is the angle of attack of the wind tunnel measurements, but the study also highlighted the fact that different numerical schemes and implementation of the hybrid model might predict buffeting at slightly higher angles. The results is therefore not surprising since SU2 is a second order solver and has been running with Roe scheme. Further, calculations have been run with a time step of 10^{-5} seconds, which is higher than what the other investigators have used.

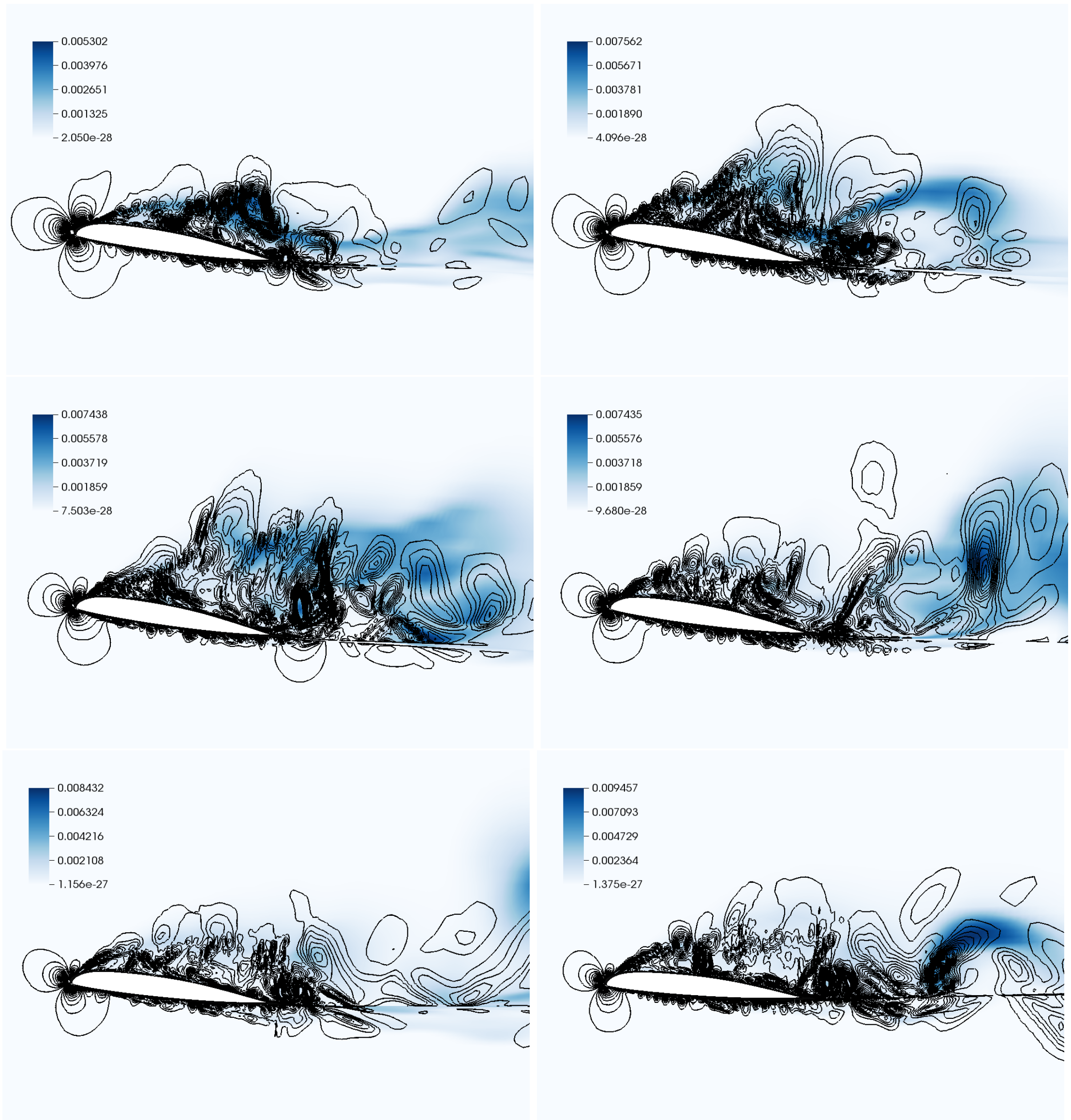

Figure 3: Visualization of flow patterns at six different times across stall by means of eddy viscosity (as calculated by the underlying RANS (SA) model) and vorticity contours. Results obtained from SA-DDES calculations.

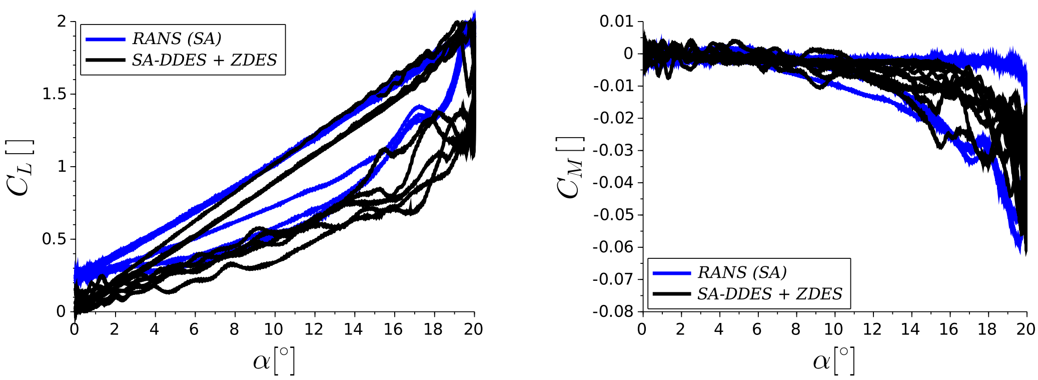

Figure 4: VR12 aerofoil, dynamic stall. Lift and pitch moment coefficients.

Second AIAA Aeroelastic Prediction Workshop, Test Case 3

Previous Results Obtained by the Author

This section summarizes the findings obtained by the author in a series of calculations spanning more than two years, two solvers and several grids. The flow appears to be much more sensitive

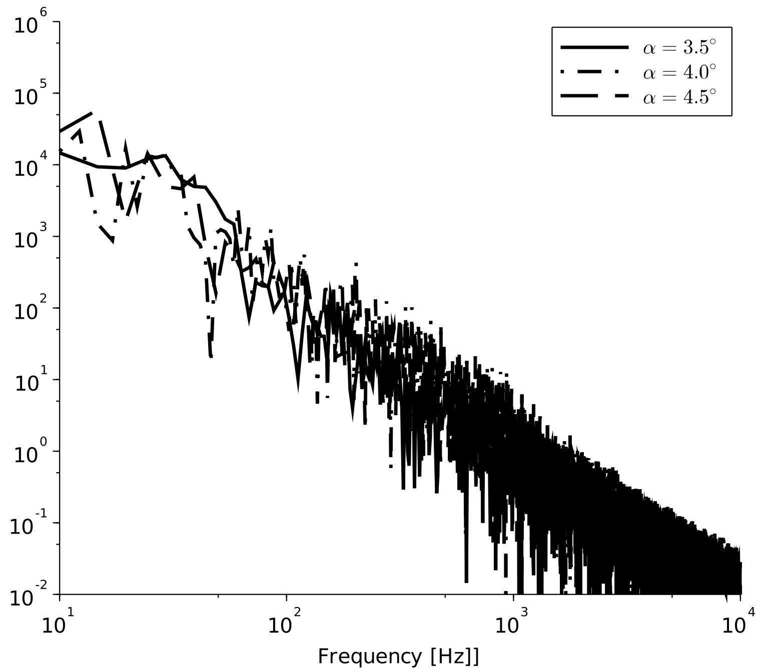

Figure 5: OAT15A aerofoil, shock buffeting. PSD calculated from lift coefficient.

to resolution than in the first example presented in section 3.3.

This test case was presented at Scitech2015 [24] as part of the Second AIAA Aeroelastic Prediction Workshop. It involves the NASA supercritical wind tunnel model BSCW [28], at Mach 0.85 and 5 degrees angle of attack. Three subcases were proposed: unforced oscillations (aimed at capturing shock buffeting), forced oscillations at 10 Hz (which correspond to a rather low reduced frequency of 0.1) and prediction of flutter speed with the wing model attached to the so-called PAPA apparatus which provides a “classical” pitch-and-plunge attachment. Note that the wind tunnel model is “very stiff” and can be considered as rigid.

The author calculated the three subcases a first time using the RANS approach [29] and subsequently checked out the SA-DDES model available with the solver Edge [30, 31]. Despite the fact that no RANS-LES specific grids were used (all calculations were carried out with the unstructured grids provided by the workshop organizers) and that the time step had not been set as a function of (the amount of) resolved turbulence (one wished to resolve), the calculations showed an evident quality improvement from RANS to SA-DDES. Response to forced oscillations is presented in Figures 7 and 8.

Subsequently, the author carried out the same calculations with the solver SU2, this time improving spatial resolution but not temporal resolution. Moreover, the SA-DDES model was implemented in SU2 [14][2] with the inclusion of the “gray-area mitigation” proposed by Deck [21], as mentioned in section 3.1. Response to forced oscillations are shown in Figures 9 and 10 and reveal a substantial difference between calculation and measurement.

The comparison with the previous Edge results is disappointing as the newer results seem more

[2]Details of the implementation can be found in IFASD2017 Paper N. 134.

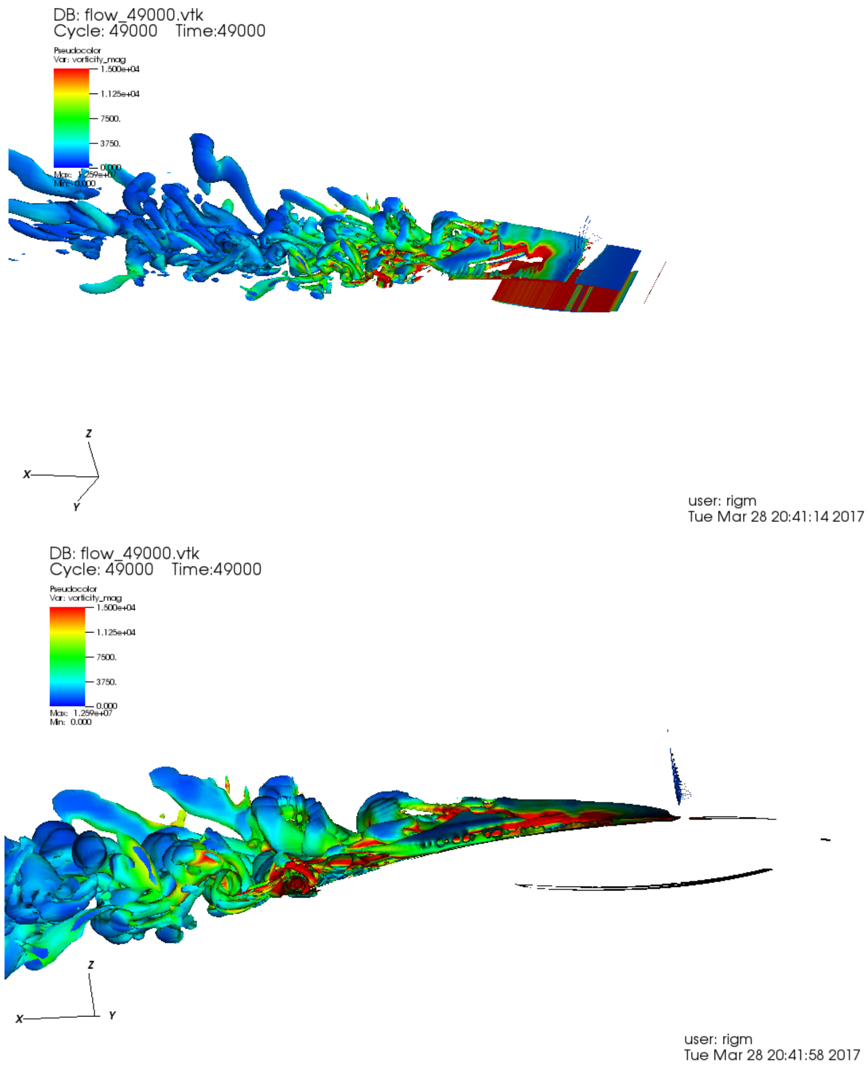

Figure 6: OAT15A aerofoil, shock buffeting. Resolved turbulent structures highlighted by the Q-criterion.

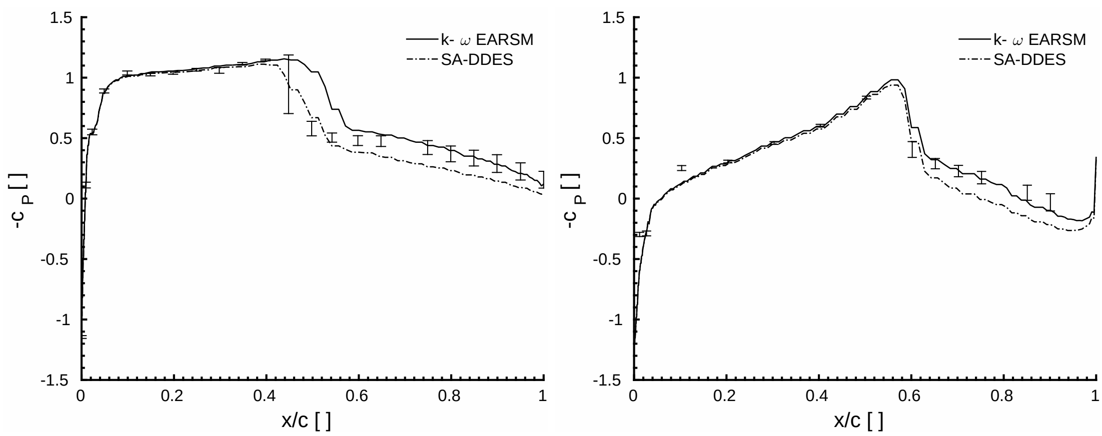

Figure 7: Time-averaged pressure distribution, calculated by Edge, from [32].

distant from the experiment. However, as a new set of calculations on finer grids are running as this paper is submitted, the following conclusions can be drawn:

1. Edge results were good as a result of a particularly good combination of spatial and temporal resolution - albeit not the ones a typical hybrid calculation would have required;

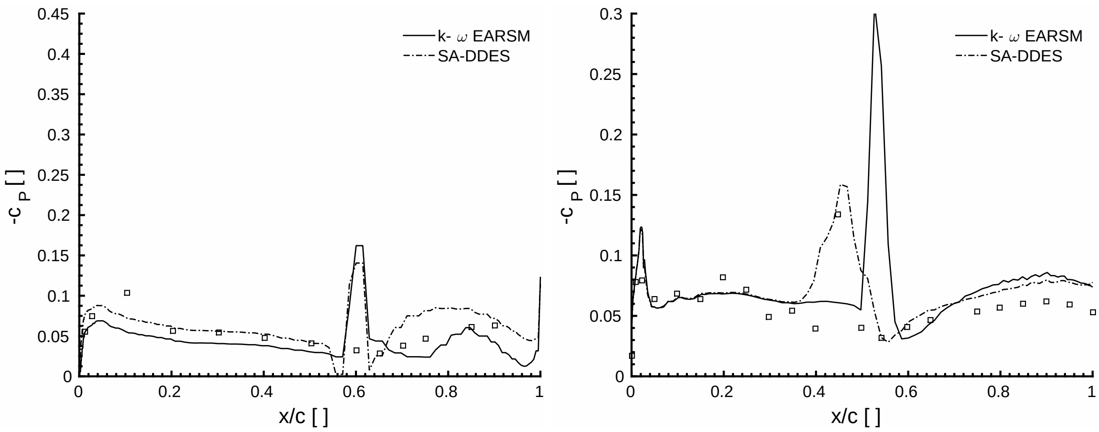

Figure 8: FRF, pressure coefficient, calculated by Edge, from [32].

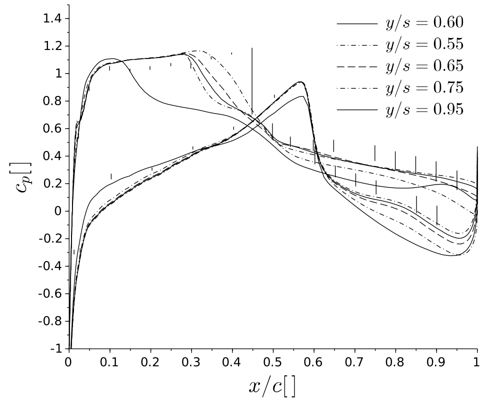

Figure 9: Time-averaged pressure distribution, calculated by SU2.

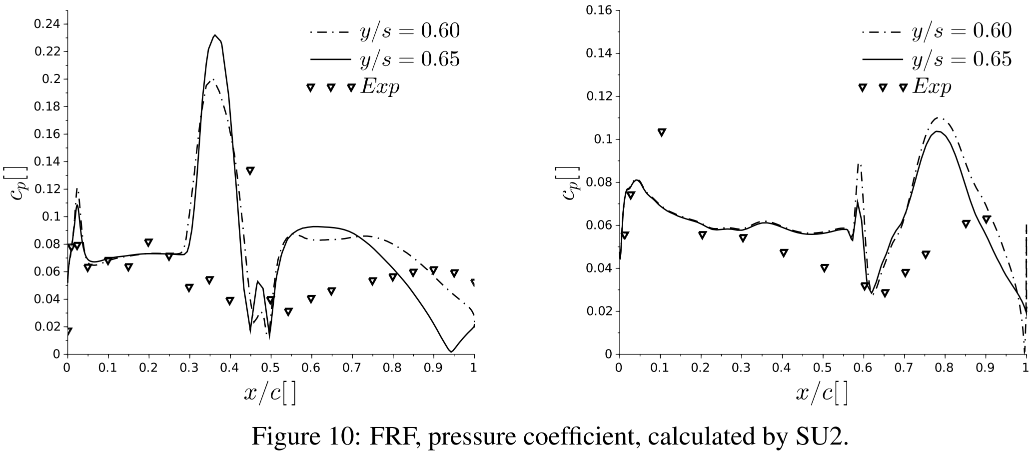

Figure 10: FRF, pressure coefficient, calculated by SU2.

in other words, even though underresolved, the hybrid model could improve the shock-boundary layer interaction.

2. SU2 results suffer from insufficient temporal resolution and hence insufficient resolved turbulence; pressure fluctuations at 10 Hz in the recovery region downstream of the shock are too high. Note that these fluctuations are not due to turbulent structures: the role of turbulence is, on the contrary, to limit them.

Following these findings, an investigation of this test case is proposed. In subsection 3.5.2 the flow patterns – generated by unforced oscillation of the fluid – obtained from calculations with different resolutions are observed and compared. In subsection 3.5.3 the response to a canonical input signal is compared. In both cases, the author wishes to quantify the effects of numerical resolution.

Analysis of Resolved Turbulent Lengthscales

Two different grids (referred to as ‘fine” and ‘coarse”) and three different time steps, for the coarse grid only, are considered. Both grids are structured; the coarse one has been generated by ICEM and has approximately 10 million elements, the finer grid has been generated by ANSA and has over 50 million elements. Both grids have been generated by E. Molina, details are available in IFASD2017 paper N. 134. Fig. 11 shows density gradients and skin friction contours obtained from coarse grid results; differences are minimal but it can be argued that a smaller time step provides finer structures. Fig. 12 shows vorticity contours from coarse grid results, providing the same impression of an additional level of detail from smaller time steps.

Vorticity and skin friction contours obtained from fine grid calculations are presented in Fig. 13. Needless to say, the difference between the turbulent structures resolved by the fine grid and those resolved by the coarse grid is substantial. Remarkably, the prediction of lift and pitch moment do not differ significantly between the different calculations.

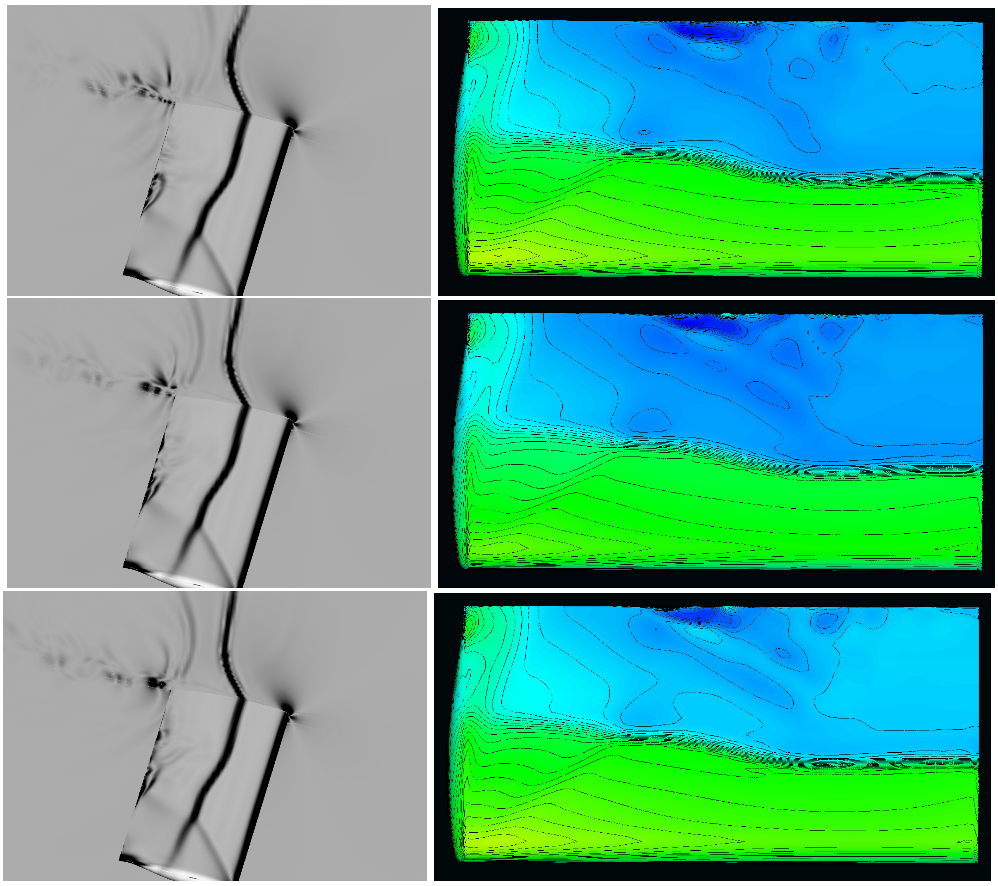

Figure 11: Visualization of flow patterns by means of density gradients (lhs) and skin friction coefficient (in freestream velocity direction) (rhs). Results obtained from SA-DDES calculations with three different time step values. From top to bottom: larger to smaller time steps.

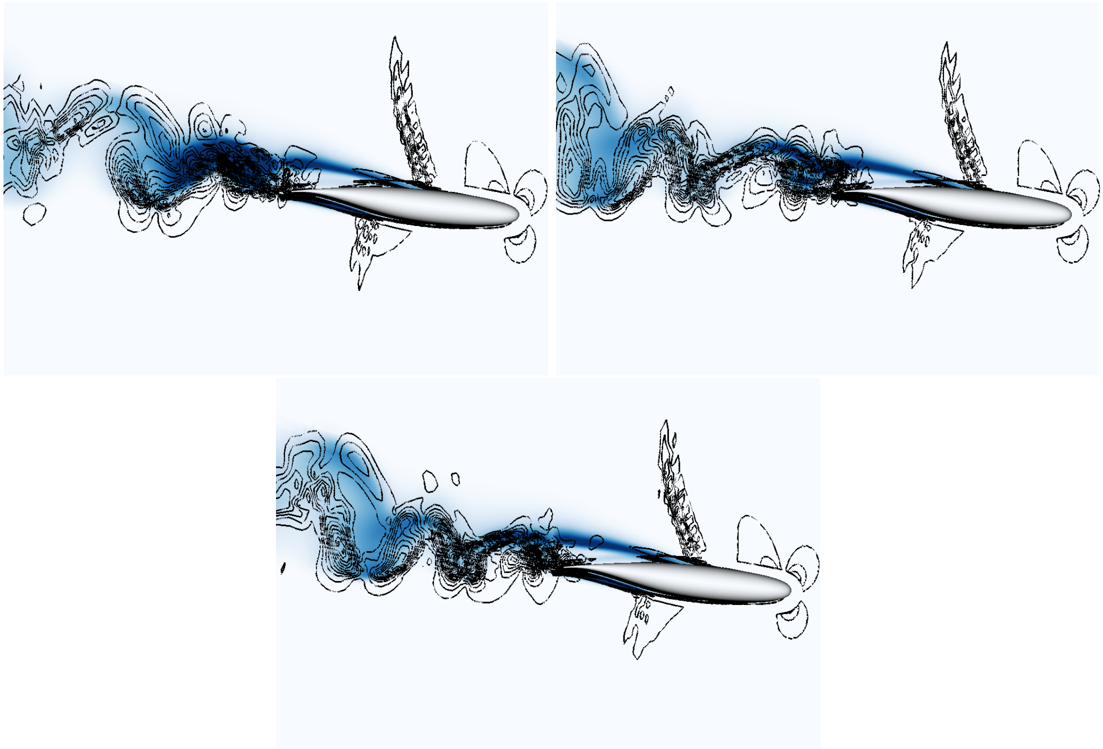

Figure 12: Visualization of flow patterns by means of vorticity magnitude and eddy viscosity (as calculated by the RANS (SA) model). Results obtained from SA-DDES calculations with three different time step values.

Sensitivity to Numerical Resolution: Response to Angle-of-Attack Step Input

An angle-of-attack step input signal is introduced at a point in time where statistical equilibrium is reached. The amplitude of the signal is approximately 2.5 degrees and it has been defined in order to strongly affect the circulation around the wing and cause a strongly non linear aerodynamic response. The response in terms of the wing lift coefficient C_L is shown in Fig. 14[3]. The differences between the various calculations are evident: surprisingly, also the impulsive parts of the response differ substantially, whereas the circulatory part of the response clearly involve different physical mechanisms depending on resolution.

Obviously such a large input signal may not be used (to train a reduced-order-model) for linear stability analysis, this is not the aim of the experiment. However, it is meaningful that differences in spatial and / or temporal resolution may lead to very different responses.

Assessment

As expected, numerical resolution plays a critical role. Even though the simulation is correctly set-up, differences in spatial or temporal resolution generate very different flow behaviours. The response to the canonical input signal is particularly significant. The conclusions may only be that no shortcuts are allowed in this case: LES must be allowed to develop properly in the separated flow regions.

[3]For a complete discussion of this type of experiment, the reader is referred to the publications by the author [33–35]

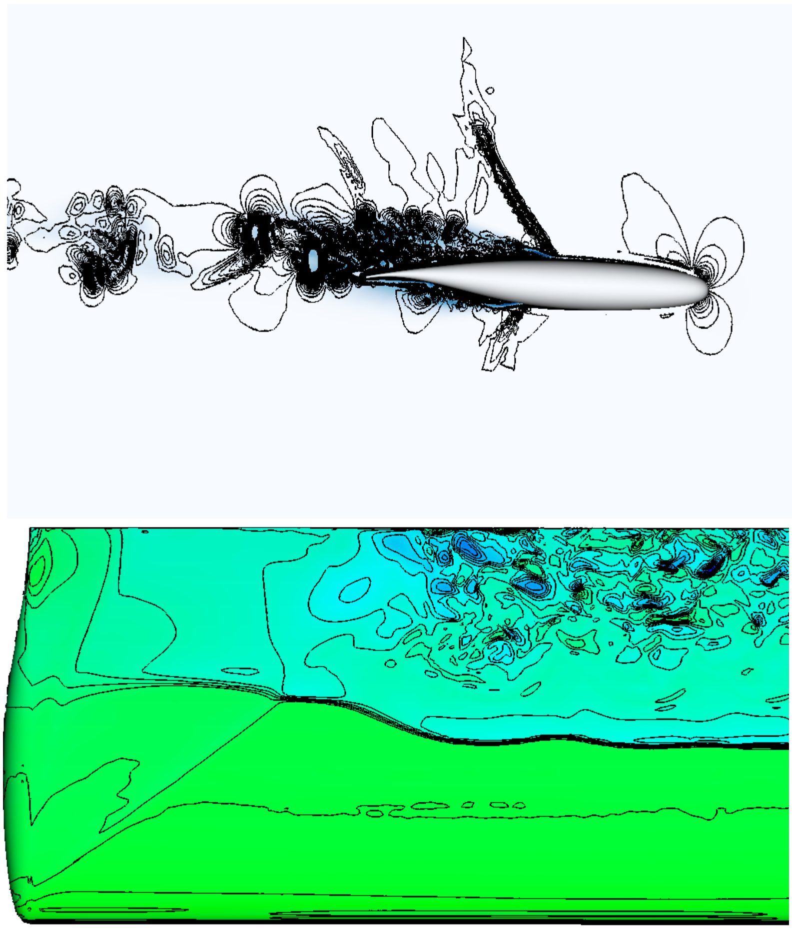

Figure 13: Visualization of flow patterns by means of vorticity magnitude and eddy viscosity (as calculated by the RANS (SA) model). Results obtained from SA-DDES calculations on fine grid

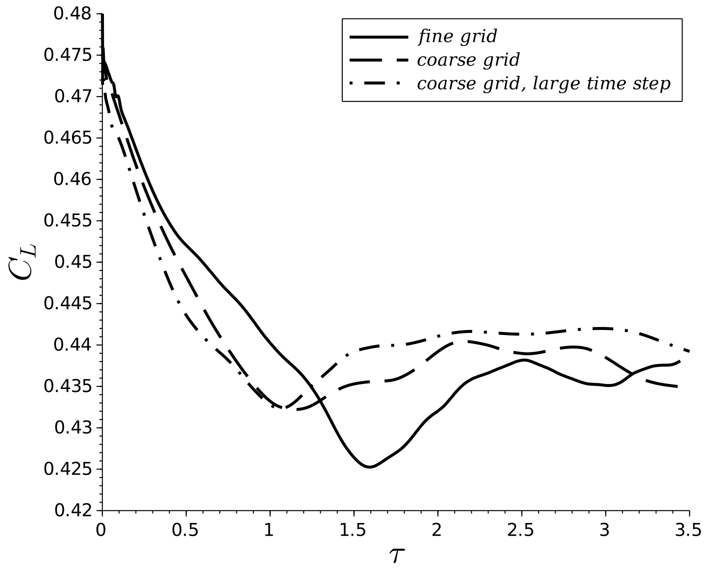

Figure 14: Response of the BSCW wing at flow conditions of Test Case 3 to a 2.5 degrees angle-of-attack step input signal. Response calculated with fine and coarse grids are shown, the latter has been calculated with two different time step lengths.

CONCLUSIONS

The statement that hybrid turbulence modelling may play a critically important role in CFD, in the near future, is undisputed. Its ability to predict flow evolution in the presence of large turbulent lenghtscales may not be matched by any RANS model. This technique is attractive also for aeroelasticians. Often, they need high-fidelity methods when linear methods fails, i.e. in the presence of aerodynamic non-linearities, possibly originated by physical phenomena which might also fall out of reach for RANS methods. This paper shows test cases, calculated with variable degree of success. However, it also provides explanations for failed calculations and hopefully demonstrates how sensitive the calculations to settings may be.

As is well known, hybrid modelling is much more expensive then RANS for many different reasons – and not only CPU. Possibly the largest efforts are those associated with preparation work, which includes the analysis of the flow, of the numerical scheme, the generation or modification of the grid and the careful set-up of the calculations. The choice of the model, its suitability to a grid and the consideration of "gray area" are also necessary steps before any investigation.

Hybrid modelling may bring along a rather drastic change in the process of CFD assessments: one which, at long last, makes understanding of flow physics mandatory.

REFERENCES

[1] Spalart, P. R. (2015). Philosophies and fallacies in turbulence modeling. *Progress in Aerospace Sciences*, 74, 1 – 15. ISSN 0376-0421. doi:http://dx.doi.org/10.1016/j.paerosci.2014.12.004.

[2] Tsinober, A. (2014). The essence of turbulence as a physical phenomenon.

[3] Spalart, P., Jou, W., Strelets, M., et al. (1997). Comments on the feasibility of les for wings, and on a hybrid rans/les approach. *Advances in DNS/LES*, 1, 4–8.

[4] Fröhlich, J. and von Terzi, D. (2008). Hybrid les/rans methods for the simulation of turbulent flows. *Progress in Aerospace Sciences*, 44(5), 349–377.

[5] Fu, S., Haase, W., Peng, S.-H., et al. Progress in hybrid RANS-LES modelling.

[6] Girimaji, S., Haase, W., Peng, S., et al. Progress in hybrid RANS-LES modelling.

[7] Peng, S. H., Doerffer, P., and Haase, W. Progress in hybrid RANS-LES modelling.

[8] Spalart, P. R. and Allmaras, S. R. (1992). A one equation turbulence model for aerodinamic flows. *AIAA journal*, 94.

[9] Spalart, P., Deck, S., Shur, M., et al. (2006). A new version of detached-eddy simulation, resistant to ambiguous grid densities. *Theoretical and Computational Fluid Dynamics*, 20(3), 181–195. ISSN 0935-4964. doi:10.1007/s00162-006-0015-0.

[10] Bendiksen, O. O. (2011). Review of unsteady transonic aerodynamics: Theory and applications. *Progress in Aerospace Sciences*, 47(2), 135–167.

[11] Heeg, J. and Chwalowski, P. (2017). Investigation of the transonic flutter boundary of the benchmark supercritical wing. In *58th AIAA/ASCE/AHS/ASC Structures, Structural Dynamics, and Materials Conference, AIAA SciTech Forum. American Institute of Aeronautics and Astronautics*, AIAA–2017–0191. doi:10.2514/6.2017-0191.

[12] Righi, M., Da Ronch, A., and Mazzacchi, F. (2017). Analysis of Resolved Turbulent Scales of Motion in Aeroelastic Problems. *AIAA-2017-0189*.

[13] Housman, J. A. and Cetin, K. C. (2017). Overset grid simulations for the second aiaa aeroelastic prediction workshop. In *58th AIAA/ASCE/AHS/ASC Structures, Structural Dynamics, and Materials Conference, AIAA SciTech Forum. American Institute of Aeronautics and Astronautics*, AIAA–2017–0640. doi:10.2514/6.2017-0640.

[14] Spode, C., Molina, E., Silva, R. G., et al. (2017). Plans and suggestions of a verification case to the aiaa aeroelastic prediction workshop. In *58th AIAA/ASCE/AHS/ASC Structures, Structural Dynamics, and Materials Conference, AIAA SciTech Forum. American Institute of Aeronautics and Astronautics*, AIAA–2017–0188. doi:10.2514/6.2017-0188.

[15] Spalart, P. R. and Streett, C. (2001). Young-person's guide to detached-eddy simulation grids.

[16] Palacios, F., Colonno, M. R., Aranake, A. C., et al. (2013). Stanford university unstructured (su2): An open-source integrated computational environment for multi-physics simulation and design. *AIAA Paper*, 287, 2013.

[17] Palacios, F., Economon, T. D., Aranake, A. C., et al. (2014). Stanford university unstructured (su2): Open-source analysis and design technology for turbulent flows. *AIAA paper*, 243, 13–17.

[18] Economon, T. D., Palacios, F., Copeland, S. R., et al. (2015). Su2: An open-source suite for multiphysics simulation and design. *AIAA Journal*, 54(3), 828–846. doi:10.2514/1.J053813.

[19] Roe, P. L. (1981). Approximate riemann solvers, parameter vectors, and difference schemes. *Journal of computational physics*, 43(2), 357–372.

[20] Venkatakrishnan, V. (1993). On the accuracy of limiters and convergence to steady state solutions. *AIAA Paper 1993-0880*.

[21] Deck, S. (2012). Recent improvements in the zonal detached eddy simulation (ZDES) formulation. *Theoretical and Computational Fluid Dynamics*, 26(6), 523–550.

[22] Martin, P., McAlister, K., Chandrasekhara, M., et al. (2003). Dynamic stall measurements and computations for a vr-12 airfoil with a variable droop leading edge. Tech. rep., DTIC Document.

[23] Deck, S. (2005). Numerical simulation of transonic buffet over a supercritical airfoil. *AIAA journal*, 43(7), 1556–1566.

[24] Heeg, J., Chwalowski, P., Schuster, D. M., et al. (2015). Plans and example results for the 2nd AIAA Aeroelastic Prediction Workshop. *AIAA Paper*.

[25] Molton, P. and Jacquin, L. (2003). Etude de l'écoulement instationnaire autour du profil transsonique OAT15A. *Rapport Technique DAAP/DAFE*.

[26] Jacquin, L., Molton, P., Deck, S., et al. (2009). Experimental study of shock oscillation over a transonic supercritical profile. *AIAA journal*, 47(9), 1985–1994.

[27] Grossi, F., Braza, M., and Hoarau, Y. (2014). Prediction of transonic buffet by delayed detached-eddy simulation. *AIAA Journal*, 52(10), 2300–2312.

[28] Dansberry, B. E., Durham, M. H., Bennett, R. M., et al. (1993). *Physical properties of the benchmark models program supercritical wing*, vol. 4457. Citeseer.

[29] Righi, M. (2016). RANS-LES Hybrid Turbulence Modelling for Aeroelastic Problems: Test Case 3 in the Second AIAA Aeroelastic Prediction Workshop. *AIAA-2016-2861*.

[30] Eliasson, P. (2001). Edge, a navier-stokes solver for unstructured grids, scientific report foi-r–0298–se. Tech. rep., Computational Aerodynamics Department, Aeronautics Division, FOI.

[31] Eliasson, P. and Weinerfelt, P. (2007). Recent applications of the flow solver edge. In *Proc. to 7th Asian CFD Conference, Bangalore, India, 2007*.

[32] Righi, M. (2016). Hybrid RANS-LES Turbulence Modelling in Aeroelastic Problems, Test Case 3 from the Second AIAA Aeroelastic Prediction Workshop. *Symposium on Hybrid RANS-LES Methods*.

[33] Berci, M. and Righi, M. (2017). An enhanced analytical method for the subsonic indicial lift of two-dimensional aerofoils – with numerical cross-validation. *Aerospace Science and Technology*, 67, 354 – 365. ISSN 1270-9638. doi:https://doi.org/10.1016/j.ast.2017.03.004.

[34] Righi, M., Koch, J., and Berci, M. (2015). Subsonic indicial aerodynamics for unsteady loads calculation via numerical and analytical methods: a preliminary assessment. *AIAA Paper No. 2015-3170*.

[35] Righi, M., Berci, M., Franciolini, M., et al. (2016). Ssubsonic indicial aerodynamics for the unsteady loads of trapezoidal wings. *AIAA Paper No. 2015-4165*.

COPYRIGHT STATEMENT